Thermal Emission-Enhanced and Optically Modulated Radioisotope Thermophotovoltaic Generators

Hongyu Wang, Xiaobin Tang, Yunpeng Liu, Zhiheng Xu, Zicheng Yuan, Kai Liu, Zhengrong Zhang, and Tongxin Jiang*

Infrared radiation generated by high-energy-density radioisotope decay can be converted to electrical energy in radioisotope thermophotovoltaic (RTPV) generators. Thermal emission intensity and spectral properties have substantial implications in this thermal energy conversion process. To improve the performance of the RTPV generator, a silicone coating material is used as a thermal emission enhancer, and SiO_2 is used as a filter. The silicone coating has excellent thermal emissivity at high temperatures. The SiO_2 filter is used for optical modulation during the thermal energy conversion process. The heat transfer optimization problem caused by the internal temperature distribution of the system is discussed. Compared with the experimental model before optimization, the output power of the RTPV generator increased by 126% obtains an open-circuit voltage of 2.64 V, an electric power of 89.88 mW, and an energy conversion efficiency of 5.62%. The RTPV generator is expected to be a potential candidate for energy supply in extreme environments.

1. Introduction

Given the increasing interest in the human exploration of the unknown, detection tasks in extreme environments, such as in deep-space, underwater, and polar environments, have grown. Specific requirements will be addressed for power systems operating in extreme environments, such as long life and high efficiency. In this context, nuclear-powered batteries present remarkable advantages in extreme environments.[1,2] Converting the energy of radioisotope decay into electrical energy is a popular topic in current research.[3–10]

Radioisotope thermophotovoltaic (RTPV) generators are devices that convert the thermal energy of isotope decay into electric energy through infrared (IR) radiation.[11] Isotopes with strong radioactivity will release a large number of high-energy rays. Some high-energy rays with weak penetrating power will deposit their own energy inside the isotope source, converting kinetic energy into heat energy. Therefore, a highly active isotope source is itself a powerful heat source, some with surface temperature of up to 1200 K or more.[12] Radioisotope usually has a long half life, plus the stability of the thermophotovoltaic (TPV) system itself,[13,14] so the RTPV has the strong potential to work long term and is stable in extreme environments.[15,16] Although the first TPV system was introduced in the 1960s,[17,18] RTPV has only begun to receive attention in recent years, the research is still in a preliminary stage.

In recent research, the design of RTPV prototypes has been mainly aimed at miniaturization in the context of special applications, such as Juha Nieminen and coworkers[19] designed an RTPV prototype with a 1000 cm^2 CubeSat size to provide power requirements for small underwater robots and deep-space equipment. General Atomics also has done extensive testing and development of a miniaturization RTPV for deep-space missions.[20] Sandia National Laboratories has designed a small-capacity radioisotope micropower system that is expected to use TPV energy conversion to generate >1 mW of electricity.[21] They only designed the prototype and were less concerned with the heat transfer optimization inside the RTPV. The numerical simulation analysis of the heat source distribution inside the RTPV by Cheon and coworkers is an improvement, but it has not been discussed experimentally.[22,23]

RTPV systems are mainly composed of a heat source, heat emitter, filter, and TPV cell (**Figure 1**). The total efficiency of the RTPV system is equal to the product of the efficiency of each part.[24] The emission performance of emitters at high temperatures is a very important consideration for RTPVs.[25] In the previous study of the emitter, researchers have also conducted extensive research on rare-Earth oxides emitters such as Er:YAG and Yb_2O_3 emitters.[26,27] After that, the researchers used photonic crystal structures with the SiO_2 and Al_2O_3 encapsulates as the emitters, they have good selective absorption and emission performance in high temperatures.[28] But they also have certain flaws. The narrowband emission of rare-Earth oxide emitters is good but the emissivity in continuous spectral bands is generally low. Also, the photonic crystal emitters are poorly tolerated for a long time at high temperatures. Modified coatings that are resistant to high temperatures and high emissivity have a better optimization and improvement of TPV conversions, such as Al_2O_3 porous medium, SiC-, Ni-, and Cr-based coatings.[29] But at this

H. Wang, Prof. X. Tang, Dr. Y. Liu, Dr. Z. Xu, Z. Yuan, K. Liu, Dr. Z. Zhang, T. Jiang
Department of Nuclear Science and Technology
Nanjing University of Aeronautics and Astronautics
29 General Road, Jiangning District, Nanjing 211106, China
E-mail: tangxiaobin@nuaa.edu.cn

The ORCID identification number(s) for the author(s) of this article can be found under https://doi.org/10.1002/ente.201901170.

DOI: 10.1002/ente.201901170

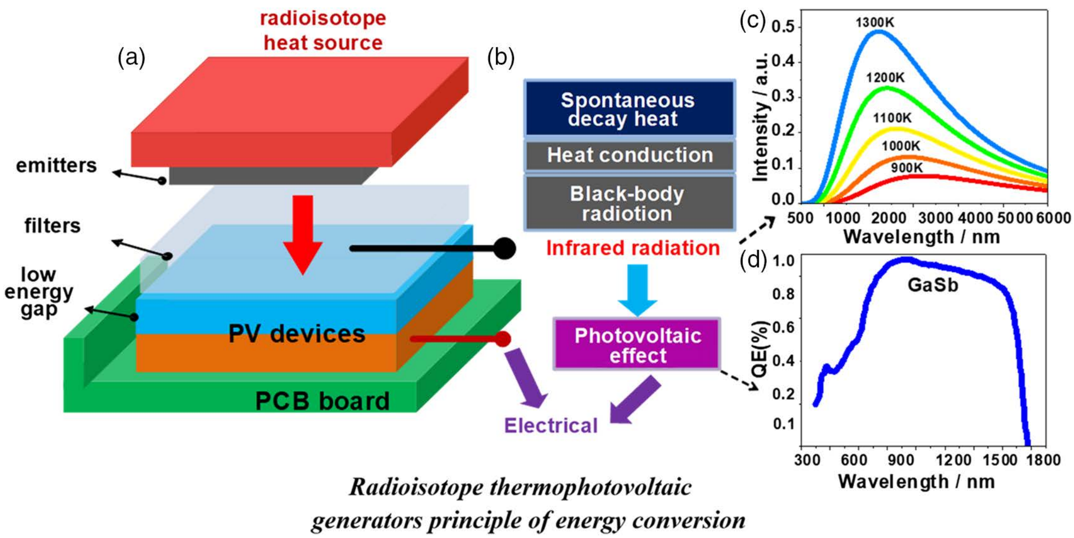

Figure 1. a) The energy conversion principle of RTPV generators with emitters and filters. b) Energy flow diagram of the battery that converts thermal with a wide integrated energy spectrum c) into an IR spectrum and eventually d) into electricity using photovoltaic devices.

time, some photons cannot be used by the TPV cell, and a large amount of waste heat will be generated. A selective filter is usually added to modulate the spectrum reaching the TPV cell, and reduce unnecessary heat transfer, it can absorb and reflects IR light in specific wavelengths, shaping the light through the filter to achieve the desired effect.[30] Adding an optical filter between the TPV cell and emitter will optimize thermal transfer process of the internal structure of RTPV.

In this work, we propose a silicone material that is easier to obtain and easy to prepare on a complex surface as an optimized emitter layer. We designed and fabricated a 300 cm^3 RTPV generator with a silicone coating thermal emission layer and a selective transmission SiO_2 filter. The radioisotope heat source is an independent source, the filter can surround the heat source as much as possible to better reduce heat loss. In this thermal transfer process, silicone coating could increase the radiation intensity of the emitter. Optical filter modulation can reduce the temperature of the TPV cell. Silicone and Al_2O_3 coatings were applied on the surface of the heat source compared with the performance changes of RTPV at different heat source temperatures. The effects of the TPV cell temperature and various electrical parameters of the RTPV system after adding the filter are discussed. Overall, the proposed methods improve the working stability and output performance of the RTPV generators and can be used to provide energy needs in extreme environments.

2. Results and Discussion

2.1. Silicone Coating Layer's Thermal Emission Enhanced

First, the current–voltage (I–V) characteristic curves of the RTPV based on the Al_2O_3 external coating heat source were tested. Based on the I–V curves of the RTPV, the output power versus voltage (P–V) was obtained. **Figure 2**a shows the experimental output performances of the Al_2O_3 external coating heat source of the RTPV at different heat source temperatures. The output power initially increases and then decreases as the voltage increases. When the heat source temperature is increased linearly from 600 K, the voltage, current, and output power also increase. When the heat source temperature is 1000 K, the entire RTPV generates an open-circuit voltage (V_{oc}) of 2.14 V, a short-circuit current (I_{sc}) of 32.82 mA, and a maximum output power (P_{max}) of 39.81 mW. The P_{max} can be calculated by Equation (1) as follows

$$P_{max} = \max(V \times I) \quad (1)$$

where V and I are the voltage and current, respectively.

Figure 2b shows the comparison of the electrical parameters of the RTPV with the silicone coating layer heat source with those of the RPTV with the Al_2O_3 external coating heat source. I_{sc} and P_{max} show a very large boost at the same heat source temperature. When the silicone coating layer heat source temperature is 1000 K, the V_{oc} and P_{max} are 2.25 V and 78.06 mW, respectively. The values of I_{sc} reached 63.61 mA.

Figure 2c shows a cross-sectional view of the original RTPV model. Silicone coating receives heat from the $^{238}PuO_2$ heat source and radiates stronger IR radiation. The outward direction is GaSb TPV cell and finned heat sink. The variation tendencies of the electrical parameters of the RTPVs as a function of the heat source temperature are shown in Figure 2d. As the temperature of the heat source increases, P_{max} and I_{sc} increase rapidly, whereas V_{oc} changes smoothly. I_{sc} and P_{max} increase slowly when the heat source temperature is within 600–800 K. At higher temperatures, I_{sc} and P_{max} increase markedly as the heat source temperature increases.

The high-emissivity performance of the silicone coating layer heat source is superior to that of the Al_2O_3 external coating heat source at the same heat source temperature. Moreover, the higher the heat source temperature, the better the performance improvement. At a heat source temperature of 1000 K, the P_{max} of the RTPV with the silicone coating layer heat source increases

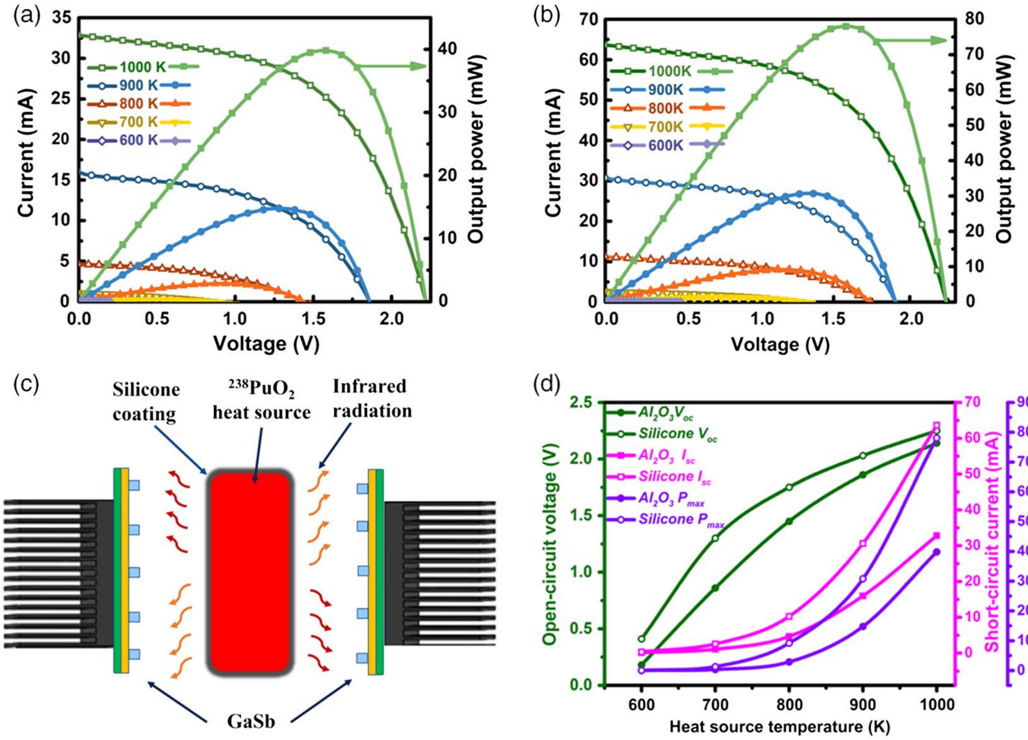

Figure 2. a) *I–V*/*P–V* curves of the RTPV with an Al_2O_3 external coating heat source, b) *I–V*/*P–V* curves of the RTPV with a silicone coating layer heat source, c) schematic of the silicone coating, d) I_{sc}, V_{oc}, and P_{max} of the different RTPV generators versus heat source temperature.

by 96.08% compared with that of the RTPV with the Al_2O_3 external coating heat source.

In the $^{238}PuO_2$ heat source temperature range (600–1000 K), the electrical properties of RTPVs show a strong dependence on the temperature of the heat source. The coating material of the heat source surface also influences the output power and energy conversion efficiency of the RTPV. Compared with those with low emissivity, heat source coatings with high emissivity provide superior RTPV performance at the same heat source temperature because more IR radiation photons are transferred to the GaSb TPV cell.

2.2. Enhanced Performance from Filters

According to the discussion in the previous section, the higher the heat source temperature, the better the electrical performance of the RTPV generator when the heat source surface temperature is between 600 and 1000 K. The temperature of the GaSb TPV cell will also increase as the heat source surface temperature increases and over time. Previous studies show that high temperatures influence the electrical performance of GaSb TPV cell. In the study of Martín and Algora and Bani et al., the V_{oc} and P_{max} of GaSb are negatively correlated, whereas I_{sc} is positively correlated with temperature.[31,32] It shows that the temperature rise will affect the output performance of the TPV cell, causing serious deterioration of the overall electrical performance of the system. Therefore, the design of simply increasing the emissivity of the emitter is not optimal, it is also necessary to control the temperature of the TPV cell. For this purpose, a filter was added to improve the performance of the RTPV generator.

A 2 mm-thick cylindrical SiO_2 filter was placed between the heat source and the GaSb TPV cell. **Figure 3**a shows a 3D model of the RTPV upon addition of the cylindrical SiO_2 filter. Figure 3b shows the RTPV model for online testing via the parameter analyzer, and Figure 3c shows a 3D diagram of the filter's regulation of IR light.

The transmittance and quantum efficiency of the GaSb cell are shown in Figure 3d. According to the quantum efficiency curve of GaSb, the transmission rate is very high in the wavelength range of 400–1600 nm. At wavelengths above 1700 nm (IR photons), however, GaSb barely produces a photovoltaic response. The energy of the photons becomes waste heat, which is deposited on the TPV cell, causing a rise in temperature. After addition of a cylindrical SiO_2 filter, most of the photons that cannot be utilized by the TPV cell are reflected, thereby reducing heat convection and radiation heat transfer to the GaSb TPV cell. Thus, the temperature of the TPV cell and the negative effects of this temperature can be significantly reduced. The temperature field balance of the RTPV heat source surface is also maintained. **Figure 4** shows the internal structure of the RTPV prototype. The silicone coating heat source is a suspension fixed on the cover. The outward portions are a SiO_2 filter, GaSb TPV cell, and finned heat sink.

We tested the Al_2O_3 external coating heat source with a cylindrical SiO_2 filter. As shown in **Figure 5**a,b, after addition of the cylindrical SiO_2 filter, the surface temperature of GaSb decreased. Compared with that of the system without the SiO_2 filter, the temperature of the surface of the GaSb TPV cell with

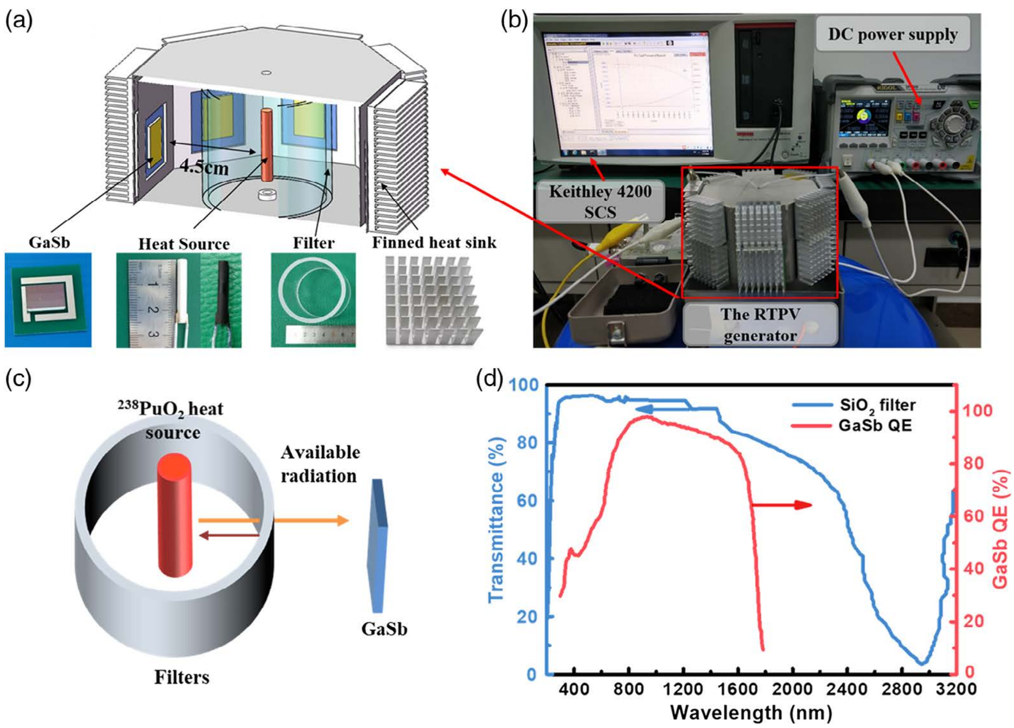

Figure 3. a) 3D model of the RTPV, b) electrical test system of the RTPV, c) diagram of the SiO_2 filter effect, and d) SiO_2 filter transmittance and GaSb quantum efficiency curves.

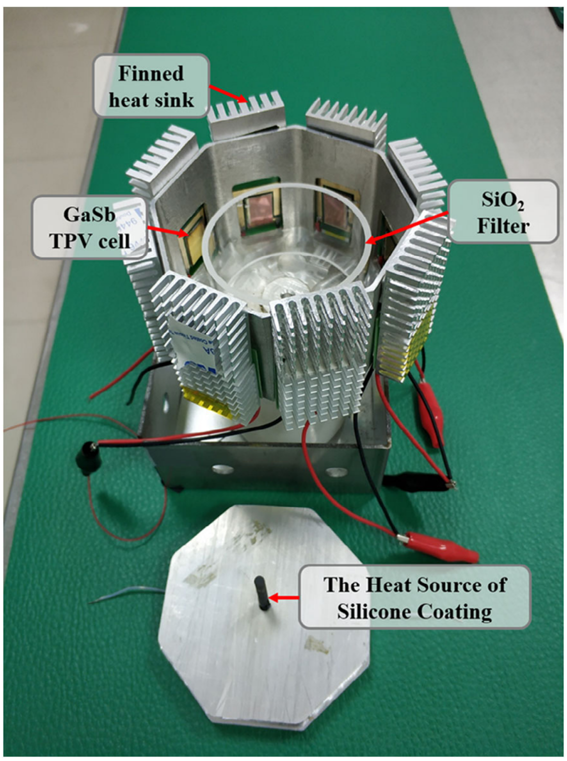

Figure 4. RTPV prototype internal display.

the SiO_2 filter is reduced by 7–12 K when the heat source temperature is within 800–1000 K, as shown in Figure 5b. The V_{oc} of this RTPV system shows significant improvement, and its I_{sc} decreases after the addition of the SiO_2 filter. This phenomenon may be attributed to two reasons. First, the SiO_2 filter can absorb or reflect some photons at 400–1700 nm, resulting in a decrease in the number of photons reaching the GaSb cell and a decrease in I_{sc}. Second, I_{sc} is positively correlated with the surface temperature of GaSb. When a filter is added, the surface temperature of GaSb is reduced, and the I_{sc} of the RTPV is decreased. When the heat source temperature is 1000 K, the output V_{oc} is 2.49 V, I_{sc} is 32.54 mA, and P_{max} is 45.55 mW in the case of the Al_2O_3-coated heat source with a SiO_2 filter. Compared with that of the system without the SiO_2 filter, the output performance of the system with the filter is improved. Specifically, the V_{oc} exhibits an upgrade of 16.3% over that without the SiO_2 filter RTPV prototype, with P_{max} upgrade of 14.4%.

The I–V and P–V curves obtained through experimental testing of the RTPV with a silicone-coating layer heat source and filter are shown in Figure 5c. Improvements in output performance as temperature increases are apparent. When the heat source surface temperature is within 800–1000 K, the surface temperature of GaSb is reduced by 9–14 K, as shown in Figure 5d. In addition, as the temperature of the heat source increases, the I_{sc} also decreases. At 1000 K heat source surface temperature, the electrical parameters of the RTPV with a silicone coating layer heat source and filter are $I_{sc} = 62.11$ mA, $V_{oc} = 2.64$ V, and $P_{max} = 89.88$ mW. Compared with the RTPV generators without SiO_2 filter, the V_{oc} of the filter-bearing system is higher by 17.33%, and its P_{max} is increased by 15.14%.

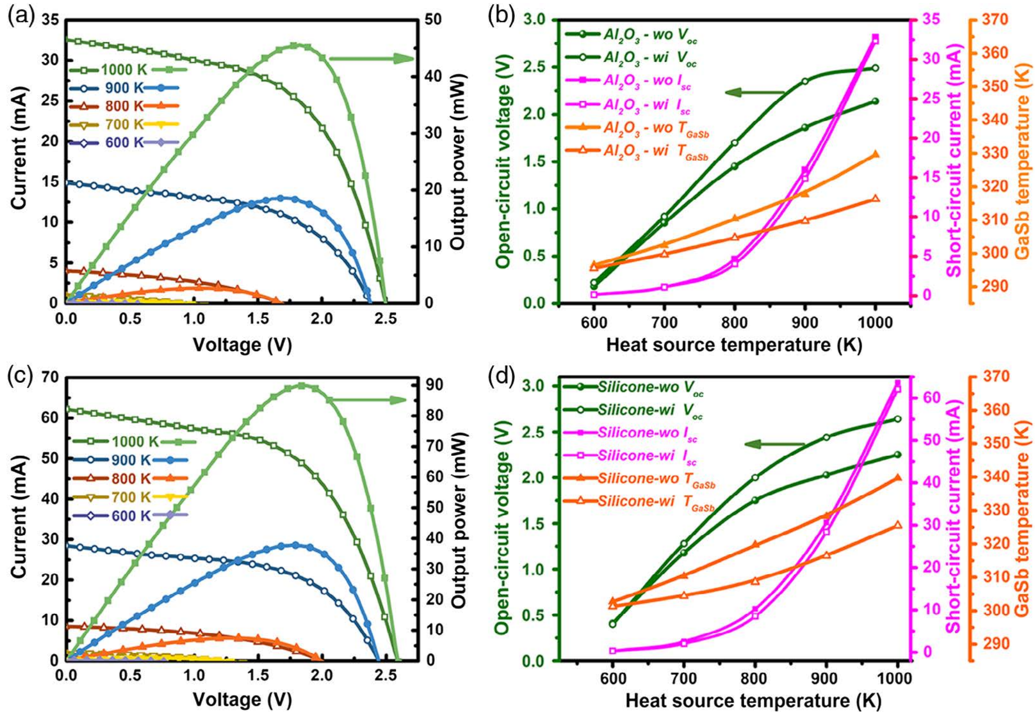

Figure 5. a,b) *I–V*/*P–V* curves of the RTPV with an Al_2O_3 external coating heat source and filter and comparison of parameters before and after addition of the SiO_2 filter, c,d) *I–V*/*P–V* curves of the RTPV with a silicone coating layer heat source and filter and comparison of parameters before and after addition of the SiO_2 filter.

2.3. Collaborative Discussions on Silicone Coating and Filters

When the heat source surface temperature is 1000 K, the electrical parameters of the four cases are as shown in **Table 1**. The effectiveness of the RTPV is calculated as follows

Adding a filter to the RTPV system can significantly improve its overall performance, and the improvement effect is more significant at high heat source temperatures (800–1000 K) than at low ones. Heat source coatings with high emissivities show better effectiveness than those with low emissivity. A high-emissivity coating and SiO_2 filter are ideal design measures for RTPV systems with improved energy conversion efficiency and performance. Compared with the experimental model before optimization, the output power of the RTPV generator increased by 126%. Considering the 10% increase in quality caused by adding filters, the power system's specific power (power/unit mass) of the RTPV generator increased by 106%. Therefore, high-emissivity coating emitters and filters are important for the optimal design and performance improvement of RTPV generators.

Table 1. Output performance comparison of the RTPV prototypes at 1000 K heat source temperature.

Coating and filter	V_{oc} [V]	I_{sc} [mA]	P_{max} [mW]	GaSb Temperature [K]
Al_2O_3-wo	2.14	32.82	39.81	329.6
Silicone-wo	2.25	63.61	78.06	339.7
Al_2O_3-wi	2.49	32.54	45.55	316.3
Silicone-wi	2.64	62.11	89.88	325.5

By enhancing thermal emission, the RTPV achieves a higher power output and energy conversion efficiency. Another way to optimize RTPV performance is the adjustment of the spectral adaptation and reduction of the temperature of the TPV cell through a filter. At the same time, we should consider that good heat dissipation can also reduce the temperature of the TPV cell, but the heat dissipation fins with 20% of mass will also reduce RTPV's specific power. The existence of a filter can reduce the temperature of the TPV cell and can replace the role of a part of the heat sink.

Ultimately, these are effective measures to adopt a selective thermal emitter and selective transmission filter to adjust the spectrum of the IR radiation to match the TPV cell, thereby reducing waste heat generation and improving the output performance of the RTPV generators.

3. Conclusions

In summary, an octahedral RTPV generator that uses a $^{238}PuO_2$ radioisotope heat source and GaSb TPV cell is prepared. Compared with radioisotope thermoelectric generators (RTGs) for current space probes, RTPV can reduce the heat source load and have a smaller mass and volume to meet the energy demands of deep-space, alpine, and deep-sea detection equipments. The thermoelectrical conversion process inside RTPV and the photothermal transport inside the system by enhancing thermal emission and spectral control are studied and optimized. The RTPV generator with a silicone coating layer can increase the radiation intensity of the heat source. The SiO_2 filter can block the heat to reach the TPV cell and lower its temperature, thereby increasing the open-circuit voltage and output power. This study demonstrates that adding a high-emissivity silicone coating layer and SiO_2 filter is a viable way to improve the performance of RTPV generators. Maintaining the balance and stability of thermal process about RTPV generator is a key factor in improving its performance. In the future, the development of new and efficient thermal coatings and spectral selection through materials for RTPV will be promising, including research on its radiation resistance and high-temperature resistance. The use of a separate wrap filter for the radioisotope heat source can better control the heat source's heat transfer and reduce heat dissipation. It will provide power supply for independent devices in the extreme environment in the near future.

4. Experimental Section

Optimized Spectrum Matching of TPV Cell: The performance of RTPVs depends on the matching of the TPV cell with the IR radiation spectrum.[33,34] Through Planck's law of blackbody radiation, we can get the blackbody IR radiation spectrum of 600–1000 K. A comparison of the spectrum with the quantum efficiency of existing photovoltaic cells is shown in **Figure 6**. The difference between the peak position of the IR radiation spectrum and the bandgap of the TPV cell can quantitatively indicate the spectral matching performance. For RTPV generators, proper coupling between the IR light and TPV cell spectral response band is required to achieve maximum conversion efficiency. The blackbody radiation power density (M), IR spectral peak position (E_{peak}), and power density (E_d) are calculated by Equation (2)–(4) as follows

$$M(\lambda) = \frac{2\pi hc^2}{\lambda^5 \left(e^{\left(\frac{hc}{\lambda kT}\right)} - 1\right)} \tag{2}$$

$$E_{peak} = \frac{hcT}{b} \tag{3}$$

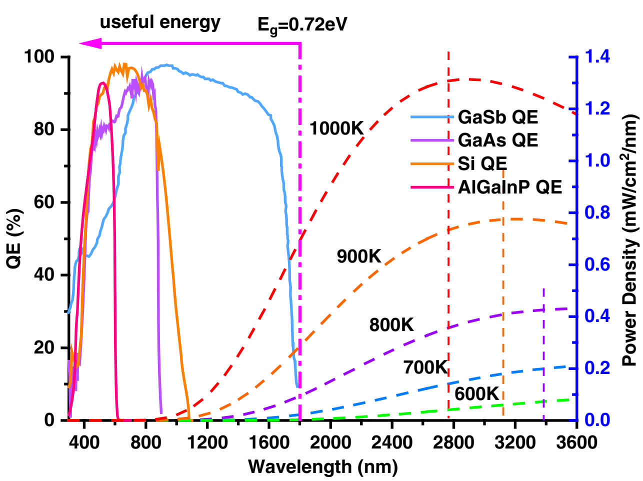

Figure 6. Spectrum of blackbody emission at 600–1000 K. The wavelength corresponding to the emission peak is given by Wien's law. The quantum efficiency curves of different photovoltaic cells are shown to compare with the blackbody emission spectrum.

$$E_d = \int_0^\infty \varepsilon Q(\lambda) M(\lambda) d\lambda \tag{4}$$

where h is Planck's constant, k is Boltzmann constant, c is the speed of light, T is the surface temperature of heat source, λ is the IR spectrum wavelength, b is Wien's displacement constant, ε is the surface emissivity, and Q is the quantum efficiency curve of the TPV cell.

Earlier TPV systems used Si as a TPV cell, and the bandgap width was 1.12 eV. According to Wien's displacement law, the IR spectral peak position difference with the 1000 K blackbody is 0.692 eV (E_{peak}). Numerical calculations reveal that the output power density (E_d) is 3.85 mW cm^{-2} (the blackbody's emissivity $\varepsilon = 1$). Gallium antimonide (GaSb JX Crystals Inc.) TPV cells have been extensively studied in the field of TPV research due to their excellent performance in IR photon energy conversion.[35–38] As such, these devices are considered as RTPV generator energy conversion units. GaSb has a bandgap of 0.72 eV, which is 0.292 eV from the peak of the 1000 K blackbody spectrum. The calculated E_d of GaSb is 52.7 mW cm^{-2}. Compared with other photovoltaic cells, including Si, GaAs, and AlGaInP, GaSb shows better photovoltaic performance under IR radiation. Therefore, this study used GaSb as the TPV cell; this cell had an effective area of 11.05 mm × 16.51 mm, and was directly fabricated on the printed circuit board (PCB) substrate. **Figure 7** shows the prototype and internal structure schematic of the GaSb device.

Radioisotope Heat Source: Radioisotopes that can be applied to RPTV's heat sources require a long half life to ensure a long life, a high energy density to achieve high temperatures, and low penetrating radiation doses to ensure the safety of operators and powered equipment. Alternative radioisotope heat source nuclei are mainly Sr/Y-90, Am-241, and Pu-238. **Table 2** shows the main characteristics of them.[23,39] Sr/Y-90 has a high specific activity and initial specific power. The half life of 28.9 years can also maintain a long life, but the decaying daughter Y-90 has a strong beta radiation, which produces a strong secondary bremsstrahlung. The thick shield reduces its high specific power advantage. Am-241 has a half life of 432.7 years and has a great life expectancy. Its energy gamma release lower than 59.5 keV is easily shielded, but its specific power is low, making it difficult to achieve the high temperatures required for RTPV systems. The half life of Pu-238 is 87.7 years. The radioactive ray is easy to shield, has a high power density, and is widely used in current space isotope power supplies. In summary, Pu-238 is the best choice for RTPV isotope heat sources.

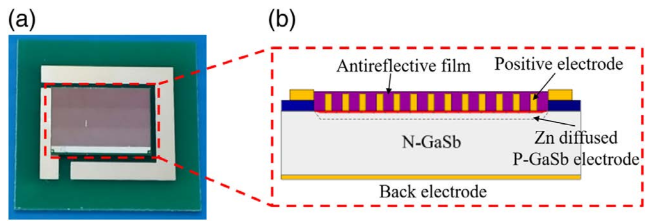

Figure 7. a) Prototype and b) internal structure schematic of GaSb device.

Table 2. Comparison of radioisotope heat source properties parameters.

	Sr/Y-90	Am-241	Pu-238
Decay ray type and average energy [MeV]	β (Sr):0.196 β (Y):0.933	α:5.48 γ:0.0595	α:5.59 γ:0.0435
Compound form	$^{90}SrTiO_3$	$^{241}AmO_2$	$^{238}PuO_2$
Half life [year]	28.9	432.7	87.7
Initial specific power [W kg^{-1}]	886.6	111.0	480.0
Initial volumetric power density [W cm^{-3}]	4.54	1.52	5.52
Specific activity [Ci g^{-1}]	133	3.43	15

Based on the heat capacity and thermal conductivity parameters of $^{238}PuO_2$,[40,41] a heat source surface temperature and heat transfer simulation model was established in COMSOL multiphysics. We obtained the surface temperature of the corresponding power ($P_{isotope}$) under the same volume of $^{238}PuO_2$ heat source with different purities, the relevant data are shown in **Table 3**. $^{238}PuO_2$ was simulated using an equivalent electric heating heat source. The cylindrical heat source designed in the experiment measured $\varnothing = 0.38$ cm and $L = 2.5$ cm.

$^{238}PuO_2$ was used as the heat source, mainly because of its long half life (87.7 years), high initial volumetric power density ($D = 5.52$ W cm^{-3}), and melting point (2700 K). The isotope can provide a long-term, efficient, and stable energy supply. The decay power of $^{238}PuO_2$ ($P_{isotope}$) is calculated as follows

$$P_{isotope} = Dp\pi L\left(\frac{\varnothing}{2}\right)^2 \tag{5}$$

where D is the initial volumetric power density of $^{238}PuO_2$, p is the $^{238}PuO_2$ proportion of heat source, L is the length of cylindrical heat source heat, and $\varnothing$ is the diameter of cylindrical heat source heat.

Emitter Optimization: Because Al_2O_3 is inexpensive and has excellent heat resistance, it is often used as a protective layer on the surface of heat emitters.[42,43] So we considered Al_2O_3 external coating as a primary comparison sample. A silicone coating with advantages in high-temperature emission was also proposed as surface coating for thermal emitters. In this study, two types of coating material sources were prepared for the RTPV prototype: an Al_2O_3 external coating heat source and a silicone coating layer heat source. Measured multiple times with a thickness gauge, the average thicknesses of both coatings were 30 μm, and the error was 1 μm. The Al_2O_3 external coating had a high-temperature tolerance, thereby ensuring the long-term and stable operation of the RTPV at high temperatures. The surface emissivity of the Al_2O_3 external coating heat source was 0.35, which was greatly improved compared with that of the iridium metal cladding ($\varepsilon = 0.05$) of GPHS $^{238}PuO_2$ pellet. The surface of the silicone coating layer heat source had an adhesion layer of silicone with an emissivity of 0.52 at high temperatures, as shown in **Figure 8**. Good IR radiation characteristics at the same heat source temperature could enhance the efficiency of RTPV systems. In this experiment, we adopted electric heating rods as simulated heat sources and controlled the surface temperature of the heat source to 600–1000 K.

The heat source view factor and the shape of the TPV cell were considered as we designed the RTPV. During radiative heat transfer, the view factor was the proportion of radiation leaving surface A to that striking surface B. The view factor accounted for the effects of orientation on radiation between surfaces. A cylindrical heat source and square GaSb TPV cell were used in the experiment, and the RTPV designed for this study was a flat octagonal prism. The middle part of the RTPV was a cylindrical radioisotope heat source. Eight GaSb TPV cells were connected in series with each other at a distance of 4.5 cm from the heat source. The outermost part was composed of a metal structure and heat radiating fins, for support and heat dissipation. The entire RTPV had a volume of ≈300 cm^3.

A programmable linear direct current (DC) power supply (DP832A, RIGOL Technologies Inc.) was used to provide a constant current source for the electric heating rod. Measurements were obtained at every 100 K as the heat source temperature was increased from 600 to 1000 K.

Table 3. Data of simulated $^{238}PuO_2$ heat sources in COMSOL.

Pellet power [W]	Pellet temperature [K]	$^{238}PuO_2$ mass [g]	$^{238}PuO_2$ proportion [%]
0.42	600	0.875	25
0.6	700	1.26	36
0.9	800	1.89	54
1.26	900	2.625	75
1.6	1000	3.5	100

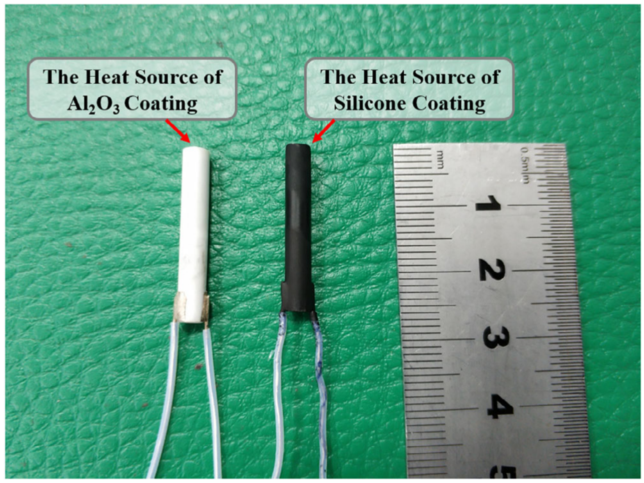

Figure 8. On the left is Al_2O_3 external coating heat source, and on the right is silicone coating layer heat source.

The electrical performances of the RTPV were tested using a parameter analyzer (Keithley 4200 SCS) in a dark environment at normal temperature (293.15 K) and standard atmospheric pressure (1 atm). The real-time temperatures of the heat source and GaSb TPV cell were measured using a temperature sensor. To minimize errors and improve the accuracy of the measurement data, tests were conducted when the internal and external temperatures of the RTPV had stabilized.

Acknowledgements

This work was supported by the National Natural Science Foundation of China (grant no. 11675076), the Jiangsu Planned Projects for Postdoctoral Research Funds (grant no. 1601139B), and the Foundation of Graduate Innovation Center in NUAA (grant no. kfjj20180606).

Conflict of Interest

The authors declare no conflict of interest.

Keywords

gallium antimonide, nuclear batteries, radioisotope thermophotovoltaic, silicone coatings, thermal energy conversions

Received: October 4, 2019
Revised: November 27, 2019
Published online: December 10, 2019

[1] M. A. Prelas, C. L. Weaver, M. L. Watermann, E. D. Lukosi, R. J. Schott, D. A. Wisniewski, *Prog. Nucl. Energy* **2014**, *75*, 117.
[2] R. G. Lange, W. P. Carroll, *Energy Convers. Manag.* **2008**, *49*, 393.
[3] Z. Xu, X. Tang, Y. Liu, Z. Zhang, C. Wang, Z. Yuan, L. Kai, *Energy Technol.* **2017**, *5*, 1638.
[4] Z. Zhang, X. Tang, Y. Liu, D. Zhou, Z. Xu, M. Wu, Z. Cao, *Energy Technol.* **2018**, *6*, 1959.
[5] J. Li, X. Tang, Y. Liu, Z. Yuan, Z. Xu, K. Liu, *Energy Technol.* **2019**, *7*, 1800707.

[6] K. Liu, Y. Liu, Z. Xu, Z. Zhang, Z. Yuan, X. Guo, Z. Jin, X. Tang, *Appl. Therm. Eng.* **2017**, *125*, 425.
[7] L. Kai, X. Tang, Y. Liu, Z. Yuan, J. Li, Z. Xu, Z. Zhang, C. Wang, *J. Power Sources* **2018**, *393*, 161.
[8] Z. Yuan, X. Tang, Z. Xu, J. Li, W. Chen, K. Liu, Y. Liu, Z. Zhang, *Appl. Energy* **2018**, *225*, 746.
[9] Z. Yuan, X. Tang, Y. Liu, Z. Xu, K. Liu, J. Li, Z. Zhang, H. Wang, *J. Power Sources* **2019**, *414*, 509.
[10] M. A. Prelas, M. T. Tchouaso, *Appl. Radiat. Isot.* **2018**, *139*, 70.
[11] D. Chubb, *Fundamentals of Thermophotovoltaic Energy Conversion*, Elsevier, Amsterdam, **2007**.
[12] G. H. Rinehart, *Prog. Nucl. Energy* **2001**, *39*, 305.
[13] X. P. Zhao, X. U. Bin, W. U. Jian, J. X. Miao, H. Xue, *Energy Technol.* **2008**, *3*, 29.
[14] Z. Utlu, U. Paral, Çağrı Gültekin, *Energy Technol.* **2017**, *6*, 1039.
[15] A. Datas, A. Martí, *Sol. Energy Mater. Sol. Cells* **2017**, *161*, 285.
[16] D. Wilt, D. Chubb, D. Wolford, P. Magari, C. Crowley, in *AIP Conf. Proc.* **2007**, *890*, 335.
[17] D. C. White, B. D. Wedlock, J. Blair, in *15th Annu. Proceedings, Power Sources Conf.*, **1961**, pp. 125–132.
[18] B. D. Wedlock, *Proc. IEEE* **1963**, *51*, 694.
[19] J. Khatry, J. Nieminen, J. Smith, K. Slotten, Nuclear and Emerging Technologies for Space (NETS-2017), Orlando **2017**.
[20] J. E. Strauch, A. Klein, P. Charles, C. Murray, M. Du, in *Proc. of Nuclear & Emerging Technologies for Space (NETS 2015)*, Albuquerque, NM **2015**, 366.
[21] R. D. Koudelka, C. S. Murray, J. G. Fleming, M. J. Shaw, V. Teofilo, C. Alexander, in *AIP Conf. Proc.* **2006**, *813*, 545.
[22] J. Lee, S. J. Cheon, S. Hong, Y. Nam, *Int. J. Heat Mass Transf.* **2017**, *108*, 1115.
[23] S. J. Cheon, S. G. Hong, J. H. Lee, Y. S. Nam, *Int. J. Energy Res.* **2018**, *42*, 817.
[24] C. Ferrari, F. Melino, M. Pinelli, P. R. Spina, *Appl. Energy* **2014**, *113*, 1717.
[25] T. Bauer, *Thermophotovoltaics: Basic Principles and Critical Aspects of System Design*, Springer Science & Business Media, Cham, Switzerland **2011**.
[26] W. J. Tobler, W. Durisch, *Appl. Energy* **2008**, *85*, 483.
[27] B. Bitnar, W. Durisch, R. Holzner, *Appl. Energy* **2013**, *105*, 430.
[28] D. Jiang, W. Yang, *Appl. Therm. Eng.* **2017**, *125*, 1253.
[29] A. K. Ismail, M. Z. Abdullah, M. Zubair, A. R. Jamaludin, Z. A. Ahmad, *J. Energy Inst.* **2016**, *89*, 81.
[30] H. Wang, S. Kaur, M. Elzouka, R. Prasher, *Appl. Therm. Eng.* **2019**, *153*, 221.
[31] D. Martín, C. Algora, *Semicond. Sci. Technol.* **2004**, *19*, 1040.
[32] S. Bani, J. Pan, A. Tang, Q. Lu, Y. Zhang, *Appl. Therm. Eng.* **2018**, *129*, 596.
[33] B. Davenport, S. Michael, in *A Collection of the 22nd AIAA Int. Communications Satellite Systems Conf. and Exhibit Technical Papers* **2004**, *2*, 1299.
[34] Z. Yang, J. Wang, X. Chen, G. Lin, *Environ. Prog. Sustain. Energy* **2017**, *37*, 513.
[35] A. S. Vlasov, V. P. Khvostikov, S. V Sorokina, N. A. Potapovich, V. S. Kalinovskiy, E. P. Rakova, V. M. Andreev, A. V Bobyl, G. F. Tereschenko, *Semiconductors* **2010**, *44*, 1244.
[36] L. Tang, Y. Hong, J. Xu, *Sol. Energy Mater. Sol. Cells* **2014**, *122*, 94.
[37] L. Tang, L. M. Fraas, Z. Liu, H. Duan, X. Chang, *IEEE Trans. Electron Dev.* **2017**, *64*, 5012.
[38] L. Fraas, J. Samaras, J. Avery, L. Minkin, in *Conf. Rec. IEEE Photovoltaic Spec. Conf.* **2000**, 1020.
[39] X. Wang, R. Liang, P. Fisher, W. Chan, J. Xu, *Renew. Sustain. Energy Rev.* **2019**, 109572.
[40] T. Arima, S. Yamasaki, Y. Inagaki, K. Idemitsu, *J. Alloys Compd.* **2005**, *400*, 43.
[41] O. L. Kruger, H. Savage, *J. Chem. Phys.* **1968**, *49*, 4540.
[42] D. Woolf, J. Hensley, J. G. Cederberg, D. T. Bethke, A. D. Grine, E. A. Shaner, *Appl. Phys. Lett.* **2014**, *105*, 81110.
[43] M. C. Mesa, P. B. Oliete, R. I. Merino, V. M. Orera, *J. Eur. Ceram. Soc.* **2013**, *33*, 2587.

